Spectral and spatial emission characteristics of edge-emitting InGaAs/GaAs quantum well laser diodes featuring an ultra-broad optical waveguide

© A.A. Beckman¹, I.A. Melnichenko^{2,3}, Yu.M. Shernyakov¹, G.O. Kornyshov¹, N.Yu. Gordeev¹, A.S. Payusov¹, O.I. Simchuk², Yu.S. Tkach², M.V. Maximov²

second-order mode and from the excited state on the fundamental mode.

194021 St. Petersburg, Russia

² Alferov University,

194021 St. Petersburg, Russia

³ National Research University

"Higher School of Economics",

190008 St. Petersburg, Russia

E-mail: spbgate21@gmail.com

Received April 28, 2025 Revised July 16, 2025 Accepted July 23, 2025

The laser emission spectra, far-field patterns, and near-field emission intensity distributions of InGaAs/GaAs/AlGaAs edge-emitting quantum well laser diodes with ultra-broad optical waveguide were studied as functions of the pump current and temperature. It was shown that lasing from the ground state occurs on the

Keywords: semiconductor laser diodes, vertical waveguide modes, fundamental mode, high-power laser diodes.

DOI: 10.61011/SC.2025.05.61998.8224

1. Introduction

The spatial distribution of far-field emission intensity is one of the most important characteristics of semiconductor lasers. Vertically single-mode lasers with a Gaussian far-field pattern are needed for traditional applications. However, as the range of applicability of semiconductor laser diodes expands, devices with a broad multimode vertical waveguide and a multilobe pattern may also become relevant [1,2]. Far-field control by variation of the pump current may find use in lidars with a controllable radiation pattern. The reduction in optical power density at the output mirror, which allows for a higher threshold of Catastrophic optical damage (COD) and, consequently, an increase in output power, is an important advantage of lasers with a broad vertical waveguide.

In the present study, we report the results of examination of the emission spectra and the distribution of emission intensity in the near- and far-field as functions of pump current and temperature in quantum well (QW) lasers with an ultra-broad waveguide.

2. Samples and experiment procedure

An InGaAs/GaAs/AlGaAs laser structure emitting at wavelength $\lambda \approx 1.04\,\mu\text{m}$ was grown on a n-GaAs(100) substrate by Metalorganic chemical vapour deposition. The active region, consisting of two In_{0.25}Ga_{0.75}As QWs separated by a 70-nm-thick spacer layer, was inserted at the center of an ultra-broad 2.6- μ m-thick GaAs waveguide layer.

The 1- μ m-thick n-emitter layer consisted of Al_{0.15}Ga_{0.85}As and was doped with silicon; the p-emitter layer doped with zinc had similar composition and thickness. Figure 1, a shows the scanning electron microscopy image of the cleaved facet of fabricated laser diodes with the layer thicknesses indicated. The refraction index profile of the structure under study and the calculated profile of its vertical modes (fundamental mode and second-order mode) are presented in Figure 1, b. The waveguide thickness was selected to support four vertical optical modes (0, 1, 2, and 3); its width was slightly below the cutoff for the fourth-order mode generation. First- and third-order mode lasing was made impossible by a negligibly small Γ -factor.

Stripe lasers with a contact width of $50\,\mu\mathrm{m}$ and different cavity lengths were obtained from epitaxial wafers via standard post-growth processing and cleaving. The samples were mounted with the p-contact facing up onto copper heatsinks with indium solder. To suppress the influence of self-heating, measurements were performed in the pulsed regime. Differential quantum efficiencies were determined based on the results of measurements of light-current characteristics of lasers with different cavity lengths and then used to calculate internal optical losses and the internal quantum efficiency, which were to $1.3\,\mathrm{cm}^{-1}$ and $77\,\%$, respectively.

Data on laser optical modes may be obtained both from the measurements of far-field patterns (radiation patterns) [3] and from the near-field emission distribution via near-field scanning optical microscopy (NSOM) [4]. Far-field patterns were recorded using a setup discussed

¹ loffe Institute,

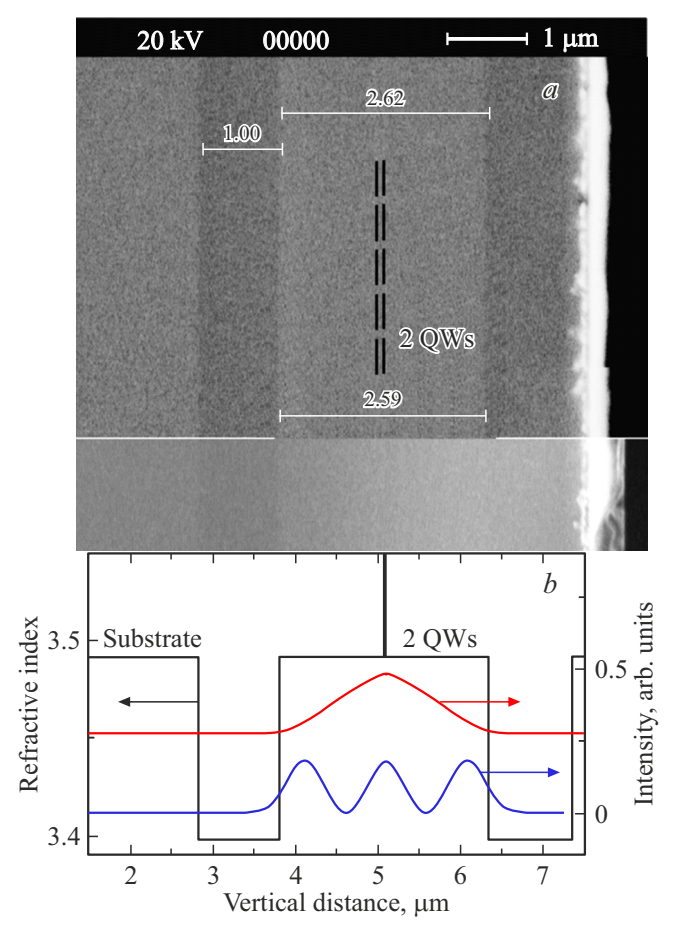


Figure 1. Laser structure under study imaged with a scanning electron microscope in the reflected (top) and secondary (bottom) electron regimes (a) and refraction index profile and calculated intensity distribution of the fundamental mode (red curve) and the second-order mode (blue curve) (b).

in detail in [5]. It featured two Standa angular motorized positioners providing rotation in two mutually perpendicular planes. The near-field of the laser diode was examined by fiber NSOM. An NT-MDT Integra Spectra II system with a fiber probe was used to scan the surface. Nufern 980-HP single-mode optical fiber mounted on a fork-shaped quartz resonator served as a probe.

3. Results and discussion

Figure 2 shows the watt-ampere characteristics of the laser diode 1 mm in length at a temperature of $20\,^{\circ}\text{C}$ (panel a) and $60\,^{\circ}\text{C}$ (panel b) obtained by integrating the electroluminescence spectra in two spectral ranges. The line at $1020-1031\,\text{nm}$ corresponds to ground state (GS) emission, while the line at $986-998\,\text{nm}$ represents excited state (ES) emission. The effect of two-state lasing is well studied in lasers based on both quantum dots (QDs) and quantum wells [6-8]. The absolute optical power values of the individual spectral components were determined

by accounting for the independently measured differential efficiency at the initial stage of GS lasing. At a low injection level, lasing is initiated at the GS optical transition with a threshold of $0.32\,\mathrm{A}$ and an emission wavelength of $\sim 1030\,\mathrm{nm}$. When the current increases to $2\,\mathrm{A}$, an emission line emerges and grows in the short-wave part of the spectrum (at $\sim 995\,\mathrm{nm}$). This line is related to the transition associated with the ES state. The intensity of GS lasing first increases with increasing current (see Figure 2,a), but starts to decrease at currents above $2.5\,\mathrm{A}$ [9]. However, it does not fall to zero within the studied current range at $20\,^{\circ}\mathrm{C}$. The intensity of ES lasing increases monotonically with current. With an increase in temperature to $60\,^{\circ}\mathrm{C}$, the GS lasing threshold goes up to $0.7\,\mathrm{A}$, while the ES lasing threshold decreases to $0.9\,\mathrm{A}$. At this temperature level, the intensity

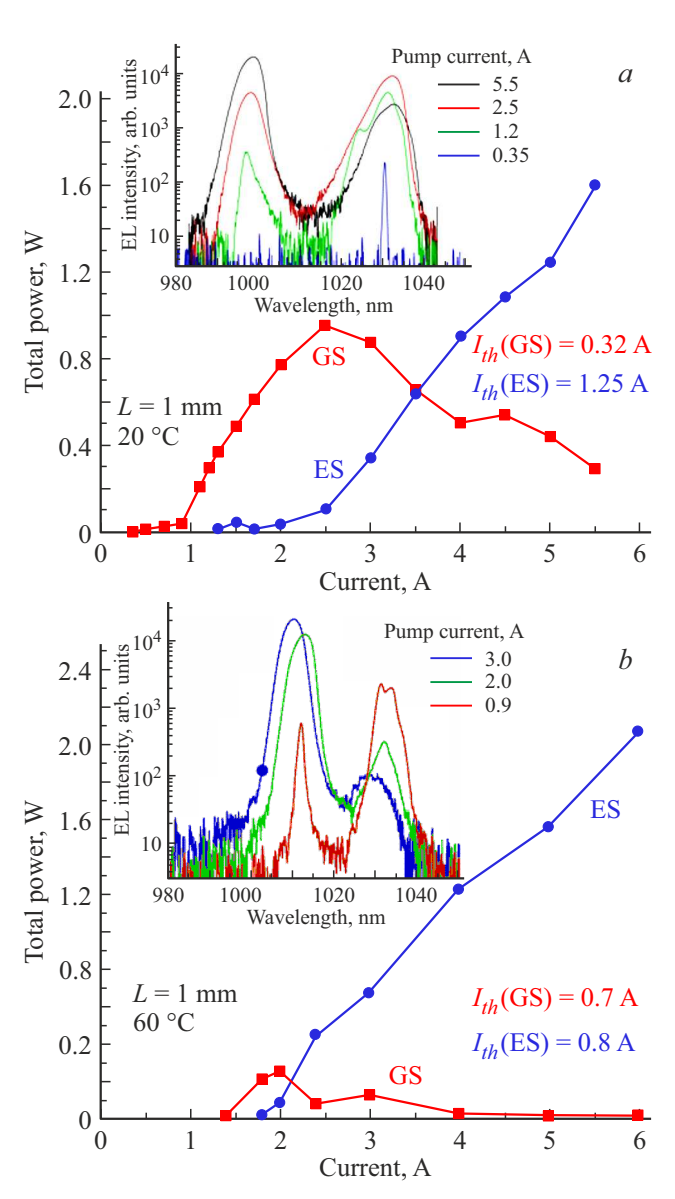


Figure 2. Watt-ampere characteristics of the laser with a 1 mm cavity at a temperature of 20 (a) and 60 $^{\circ}$ C (b). The corresponding emission spectra are shown in the insets.

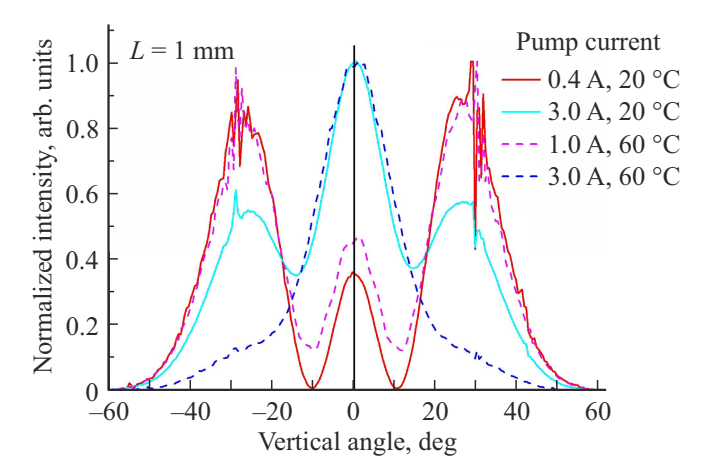


Figure 3. Far-field patterns at different pump currents and temperatures.

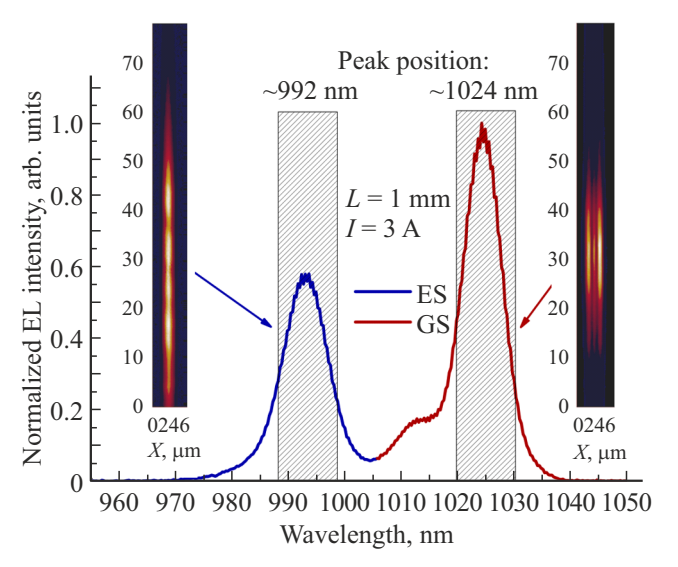


Figure 4. Room-temperature electroluminescence spectrum of the laser diode at a pump current of 3 A. Distributions of intensity at the mirror obtained in different spectral ranges are shown in the insets.

of GS emission drops almost to zero as the current increases further following the onset of ES lasing (at 3 A, GS emission is 2 orders of magnitude weaker than ES emission).

Far-field patterns were examined within the current range of 0.3-3.3 A and at temperatures of 20-60 °C. The distributions of emission intensities in the far-field corresponding to several values of current and temperature are shown in Figure 3. It can be seen that the central peak of the intensity distribution grows with increasing current, while the intensity of side peaks decreases; i.e., lasing switches from the second-order mode to the fundamental mode. It is important to emphasize that such emission mode switching is accompanied by a switch in lasing from the ground state to the excited one. A study of the temperature dependence of the far-field revealed an even more pronounced emission

peak in the central part at high temperatures and an almost complete lack of peaks around the angles of $\pm 30^{\circ}$. We associate this mode switching at stronger currents with an increase in concentration of nonequilibrium carriers in the waveguide and, consequently, with a faster growth of optical losses for high-order modes [10]. The measured mode profiles of lasers are very close to those simulated and presented in Figure 1.

The emission intensity distributions of lasers in the nearfield were also investigated at different currents via fiber NSOM. A complex pattern indicative of generation of highorder modes in both vertical and lateral directions was obtained. As the pump current increased, the laser emission intensity distribution in the vertical direction changed. The spectrum recorded using a fiber probe (Figure 4) features two intensity peaks corresponding to GS and ES lasing. The regime of spatially resolved emission spectra measurements was used to determine the mode composition of radiation corresponding to GS and ES lasing lines. Figure 4 (left inset) shows the near-field pattern corresponding to the 986–998 nm part of the spectrum (ES lasing). A single intensity band in the vertical direction, which corresponds to the fundamental vertical mode, is seen clearly. Figure 4 (right inset) shows the emission intensity distribution within the 1020–1031 nm range (GS lasing). Three intensity peaks, which represent the second-order vertical mode, are seen in the near-field in this case. Thus, second-order and fundamental modes correspond to ground-state and excitedstate lasing, respectively, in the studied lasers with an ultrabroad waveguide. The experimentally measured near- and far-field patterns are consistent with the results of calculation of the optical modes of the waveguide that are presented in Figure 1.

4. Conclusion

The near- and far-field emission intensity distributions in InGaAs/GaAs/AlGaAs quantum well lasers with an ultra-broad vertical waveguide were investigated. It was established that a change in pump current or temperature may lead to a change in spatial distribution of emission intensity due to switching between vertical modes and spectral lasing lines corresponding to the ground and excited states of the active region. It was also demonstrated for the first time that excited-state lasing proceeds in the fundamental vertical mode. This effect was observed at 60 °C, which corresponds to the standard operating regime of semiconductor lasers. A high optical gain and rapid relaxation of carriers from the waveguide to excited-state levels in QD-based lasers operating in the ES regime lead to an increase in the maximum frequency of direct current modulation (compared to lasers operating in the GS regime; see [11,12]). The same patterns are likely to apply to QW lasers, making them promising candidates for application in high-speed optical communication systems. with an ultra-broad waveguide have a higher threshold of catastrophic optical mirror damage (due to a lower optical power density at the mirror), which is one of the prerequisite conditions for achieving high levels of output power. Current-controlled adjustment of the emission spectrum and the radiation pattern holds promise for data transmission systems utilizing new coding methods [13].

Funding

This study was supported by grant No. 24-12-00358 from the Russian Science Foundation. O.I. Simchuk wishes to thank the Ministry of Science and Higher Education of the Russian Federation (project FSRM-2023-0010) for support of the study of cleaved faces of samples by scanning electron microscopy. I.A. Mel'nichenko wishes to thank the Fundamental Research Program of the National Research University Higher School of Economics for support of NSOM measurements.

Conflict of interest

The authors declare that they have no conflict of interest.

References

- S. Slipchenko, I. Shashkin, D. Nikolayev, V. Shamakhov,
 A. Podoskin, O. Soboleva, K. Bakhvalov, V. Kriychkov,
 N. Pikhtin, P. Kop'ev. Optics Lett., 48 (2), 203 (2023).
 DOI: 10.1364/OL.476248
- [2] N. Ammouri, H. Christopher, A. Maaßdorf, J. Fricke, A. Ginolas, A. Liero, H. Wenzel, A. Knigge, G. Tränkle. Optics Lett., 48 (24), 6520 (2023). DOI: 10.1364/OL.510521
- [3] A. Kozlowska, A. Malag. Proc. SPIE, 5120, 178 (2003). DOI: 10.1117/12.515429
- [4] A.V. Ankudinov, M.L. Yanul, S.O. Slipchenko, A.V. Shelaev, P.S. Dorozhkin, A.A. Podoskin, I.S. Tarasov. Opt. Express, 22 (21), 26438 (2014). DOI: 10.1364/OE.22.026438
- [5] S. Peled. Appl. Optics, 19 (2), 324 (1980).DOI: 10.1364/ao.19.000324
- [6] A.E. Zhukov, A.R. Kovsh, D.A. Livshits, V.M. Ustinov,
 Z.I. Alferov. Semicond. Sci. Technol., 18 (8), 774 (2003).
 DOI: 10.1088/0268-1242/18/8/310
- [7] M.V. Maximov, Yu.M. Shernyakov, G.O. Kornyshov, A.A. Beckman, F.I. Zubov, A.A. Kharchenko, A.S. Payusov, S.A. Mintairov, N.A. Kalyuzhnyy, V.G. Dubrovskii, N.Yu. Gordeev. Optics Lett., 49 (21), 6213 (2024). DOI: 10.1364/OL.532606
- [8] D.A. Veselov, K.R. Ayusheva, N.A. Pikhtin, A.V. Lyutetskiy,
 S.O. Slipchenko, I.S. Tarasov. J. Appl. Phys., 121 (16), 163101 (2017). DOI: 10.1063/1.4982160
- [9] V.V. Korenev, A.V. Savelyev, M.V. Maximov, F.I. Zubov, Yu.M. Shernyakov, M.M. Kulagina, A.E. Zhukov. Appl. Phys. Lett., 111, 132103 (2017). DOI: 10.1063/1.5004268
- [10] E.A. Avrutin, B.S. Ryvkin, A.S. Payusov, A.A. Serin, N.Y. Gordeev. Semicond. Sci. Technol., 30 (11), 115007 (2015). DOI: 10.1088/0268-1242/30/11/115007
- [11] B.J. Stevens, D.T.D. Childs, H. Shahid, R.A. Hogg. Appl. Phys. Lett., 95 (6), 061101 (2009). DOI: 10.1063/1.3193664

- [12] C. Wang, B. Lingnau, K. Ludge, J. Even, F. Grillot. IEEE J. Quant. Electron., 50 (9), 1 (2014). DOI: 10.1109/JQE.2014.2335811
- [13] M.V. Maximov, Yu.M. Shernyakov, N.Yu. Gordeev, A.M. Nadtochiy, A.E. Zhukov. Tech. Phys. Lett., 49 (3), 15 (2023). DOI: 10.21883/TPL.2023.03.55675.19450

Translated by D.Safin